J Fusion Energ (2014) 33:775–783
DOI 10.1007/s10894-014-9747-9

ORIGINAL RESEARCH

Conceptual Design and Finite Element Analysis of STR-3 Feeder for ITER

YinFeng Zhu · YunTao Song · YongHua Chen

Published online: 3 August 2014

Abstract The three structure (STR) cooling feeders of the international thermonuclear experimental reactor play an important role in removing heat loads from the coils cases of the superconducting magnets system. In this paper, the materials choice and conceptual design of STR-3 feeder are presented, then the structural analyses are performed based on the finite element method, which is used to evaluate the mechanical characteristics of STR-3 feeder. The results show that the structural design is basically reasonable, but the U bend or S bend structure near terminal box is necessary. Furthermore, the further structural optimization, reducing the heat leakage to cryopipes, radiation of composite insulation materials, overpressure protection and seismic analysis proposals are put forward.

Keywords Finite element analysis · Feeder · ITER · Structural optimization

Introduction

The ITER system includes 18 superconducting toroidal field (TF) coils and 6 poloidal field (PF) coils, a central solenoid (CS) with 6 coils, and 18 correction coils (CC) [1]. The stainless steel (SS) coils cases are used to contain the huge and powerful superconducting coils. To cool the coils cases adequately and house the instrumentation wires, 3 STR cooling feeders system are employed.

In conceptual design, STR-3 feeder consists of terminal box (TB), vacuum barrier (VB), cryostat feed through (CFT) and in-cryostat feeder (ICF). Considering no S bend box, U bends on ICF are used to reduce stress concentration, as shown in Fig. 1. Different from feeders for superconducting coils, there is no superconducting busbar inside STR-3 feeder [2–4], so there only has gravity, displacements loads, thermal loads and internal pressure during normal working condition.

Structural Conceptual Design

Materials Choice

To match the vacuum, cryogenic and strong electro-magnetic working environment, SS304L, SS316L, G10 and copper are used to develop STR-3 feeder. The physical properties of SS304L/316L and copper are listed in Tables 1 and 2. The physical properties of G10 comes from Ref. [5]. For the chosen materials, SS304L is used to develop TB, cryostat of CFT, thermal shield of CFT and containment duct of CFT. Due to high thermal conductivity, copper is used to develop thermal intercept of thermal shield inside TB. In order to reduce thermal conduction, G10 is used to develop supports for thermal shield inside TB and cold mass supports for CFT.

The thermal conductivities of SS304L/316L and G10 are listed in Fig. 2. Undoubtedly, the thermal conductivities of G10 are much lower than SS304L/316L. For the

Y. Zhu (✉)
School of Mechanical and Electrical Engineering, Anhui Jianzhu University, Hefei 230601, China
e-mail: zhuyinfeng@sohu.com

Y. Song
Institute of Plasma Physics, Chinese Academy of Sciences, Hefei 230031, China

Y. Chen
Magnet Division, Tokamak Department, International Thermonuclear Experimental Reactor Organization, 13067 St. Paul lez Durance, France

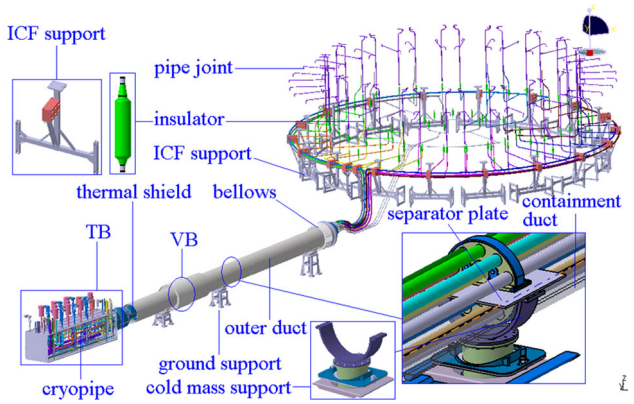

Fig. 1 3-D model of STR-3 feeder

sake of reducing thermal conduction, G10 is suitable for developing supports.

Cryopipes System Outside Terminal Box

As shown in Fig. 3, the cryopipes system outside TB mainly consists of supports, valves, bursting disc components and cryopipes. The flow of coolant inside cryopipes is controlled by valves. To protect the cryogenic system under over pressure, some bursting disc components connected to cryopipes are employed.

The venting area of bursting disc and the minimum hole diameter of holder can be calculated according to formula (1).

$$A_E \geq \frac{0.1G_v}{C \cdot K_F \cdot P}\sqrt{\frac{ZT_1}{M}} \tag{1}$$

where A_E is the venting area of bursting disc, the unit is cm^2, G_v is the maximum venting capacity of helium gas, the unit is kg/h, K_F is flow coefficient, where K_F is 0.71, P is the designed bursting pressure of bursting disc, the unit is MPa, M is the molecular weight of helium gas, where M is 4, Z is coefficient of compressibility of helium gas, T_1 is absolute temperature of helium gas inside cryopipe, the unit is K, C is characteristic coefficient of helium gas. If P is 0.2 MPa, A_E is about 20 cm^2, which corresponds to the minimum hole diameter of holder is 50 mm.

Terminal Box

From an engineering point of view, the structure of TB should be convenient for fabrication and assembly, so the shape of TB is cuboid, as shown in Fig. 4. For rectangular plate, the minimum thickness of TB can be calculated according to formula (2).

$$\delta_{\min} \geq \delta_0 + C = \frac{0.224B}{\sqrt{[\sigma]_V}} + C \tag{2}$$

where $\delta_{\min}$ is the minimum actual thickness of TB, the unit is mm, δ_0 is calculating wall thickness of TB, the unit is mm, C is additional value of wall thickness, the value is 1.5 mm, $[\sigma]_V$ is allowable bending stress, the value is 115 MPa, B is the length of narrow side of rectangular plate, the value is 1,480 mm. If there is no rib on the rectangular plate, the wall thickness of TB is 32.4 mm, to insure safety margin, the wall thickness is 40 mm.

Thermal Shield Inside Terminal Box

To reduce thermal radiation from room temperature to 4.5 K cryopipes, a 80 K thermal shield made of 3003 aluminium alloy is set inside TB. The 3-D model of thermal shield is as shown in Fig. 5. According to formula (3),

Table 1 Physical properties of SS304L/316L

Temperature (K)	4	50	100	150	200	250	293
Density (kg/m^3)	7,900	7,900	7,900	7,900	7,900	7,900	7,900
Allowable stress (MPa) (S_m) (304L)	211	147	144	139	132	123	114
Allowable stress (MPa) (S_m) (316L)	287	193	140	133	126	120	113
Young's modulus (GPa)	205	205	205	202	200	195	193
Possion's ratio	0.30	0.30	0.30	0.30	0.30	0.30	0.30
Average CTE ($\times 10^{-6}$ K^{-1})	10.21	12.05	13.5	14.48	14.99	15.02	–

Table 2 Physical properties of copper

Temperature (K)	4	10	20	50	100	273	293
Density (kg/m^3)	8,900	8,900	8,900	8,900	8,900	8,900	8,900
Young's modulus (GPa)	139	139	139	138	137	129	124
Possion's ratio	0.33	0.33	0.33	0.33	0.33	0.33	0.33
Thermal conductivity (W/m·K)	623	1,520	2,380	979	469	397	394

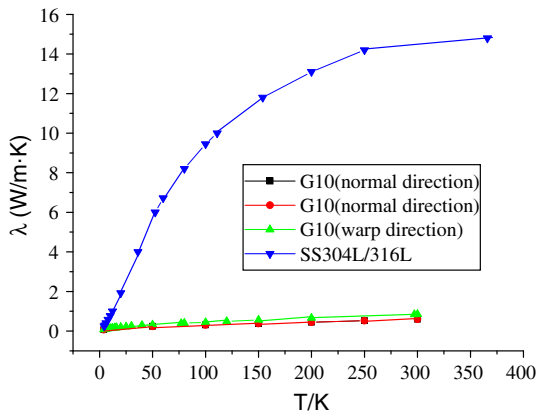

Fig. 2 Thermal conductivities of SS304L/316L and G10

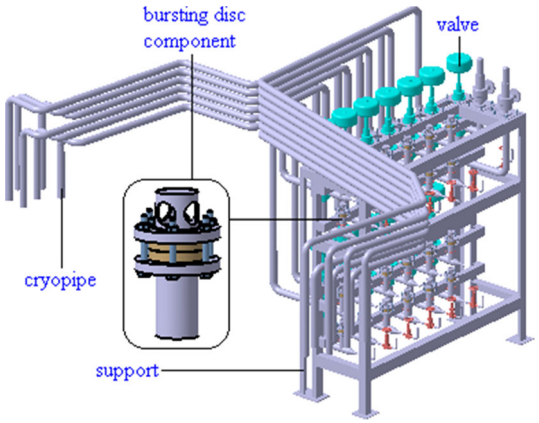

Fig. 3 3-D model of cryopipes component

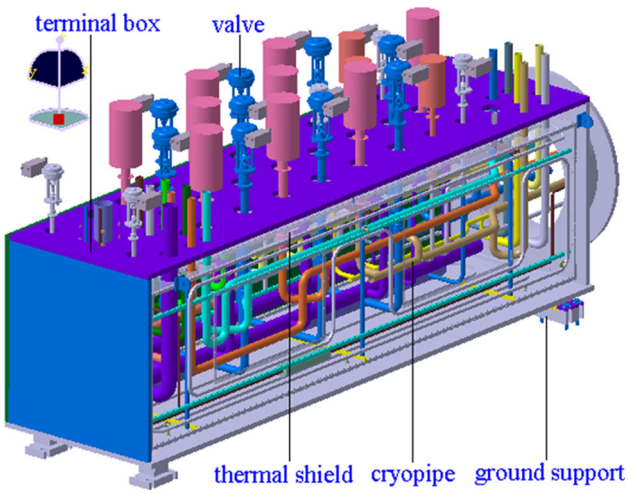

Fig. 4 3-D model of TB with inner components

if the structure and dimensions of thermal shield support are confirmed, low thermal conduction can be obtained by using material with low thermal conductivity. Therefore,

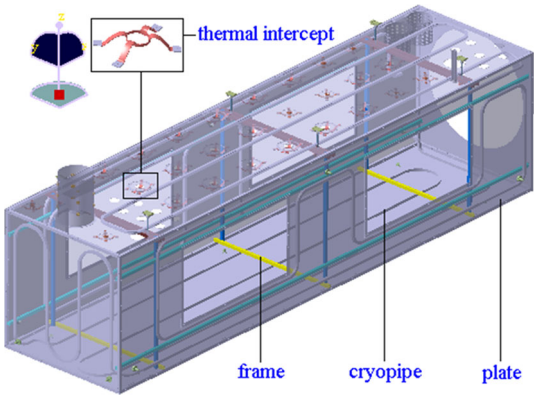

Fig. 5 3-D model of thermal shield for TB

glass fiber reinforced composite material (G10) is chosen as the structural material of thermal shield support.

$$Q = \frac{A}{L}\int_{T_2}^{T_1} \lambda(t)dt \tag{3}$$

where Q is thermal conduction through thermal shield support, A is cross section of thermal shield support, L is length of thermal shield support, T_2 and T_1 are low temperature and high temperature of thermal shield support, $\lambda(t)$ is thermal conductivity.

Due to vacuum inside TB, the thermal convection is much lower than thermal conduction and thermal radiation. If there is no multi-layer insulation on the outer surfaces of thermal shield, the thermal radiation from room temperature to thermal shield can be calculated with formula (4).

$$Q = \frac{A_1 \cdot \sigma\left[(T_1^4) - (T_2^4)\right]}{\frac{1}{\varepsilon_1} + \frac{A_1}{A_2}\left(\frac{1}{\varepsilon_2} - 1\right)} \tag{4}$$

where Q is heat flow, A_1 and A_2 are area of hot wall and cold wall, T_1 and T_2 are temperature of hot wall and cold wall, ε_1 and ε_2 are emissivities of hot wall and cold wall, σ is Stefan–Boltzmann constant, it is 5.6697×10^{-8} W/(m^2·K^4). If A_1 equals to A_2, and ε_1 equals to ε_2, formula (5) can be induced according to formula (4).

$$Q = \sigma A \frac{\varepsilon}{2-\varepsilon}\left(T_1^4 - T_2^4\right) \tag{5}$$

To reduce thermal radiation, multi-layer insulation made of glass fiber and aluminium foil can be wrapped on the outer surfaces of thermal shield. Actually, multi-layer insulation is a composite structure, as shown in Fig. 6, glass fiber is used to separate the neighbouring aluminium foil. The thermal radiation from hot wall to cold wall can be calculated with formula (6) [6].

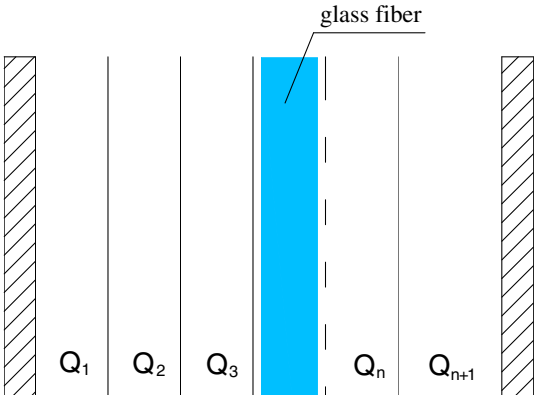

Fig. 6 Model of multilayer insulation

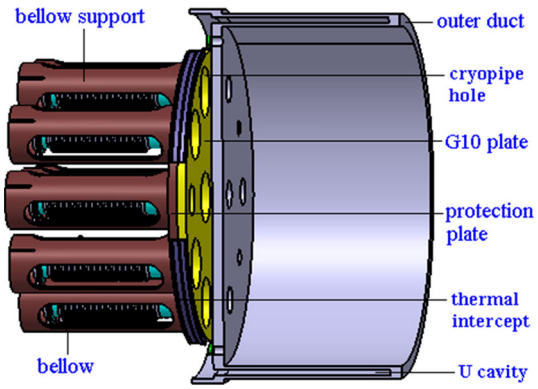

Fig. 7 3-D model of vacuum barrier

$$Q = \frac{1}{n+1}\sigma A \frac{\varepsilon}{2-\varepsilon}\left(T_1^4 - T_{n+2}^4\right) \quad (6)$$

Compared formula (5) with formula (6), it can be seen that thermal radiation of thermal shield inside TB can be reduced greatly by using multi-layer insulation.

Vacuum Barrier

VB is used to separate the TB vacuum and CFT vacuum, so STR-3 feeder maintains two different vacuum systems. To reduce thermal conduction from room temperature, U cavity structure is designed for outer duct. Considering displacements during cool down and warm up, bellows are used to compensate the axial displacements of cryopipes, in addition, the thermal resistance between cryopipes and outer duct are increased by using bellows. The 3-D model of VB is as shown in Fig. 7.

Cold Mass Support on CFT

The 3-D model of cold mass support is as shown in Fig. 8. Due to no busbar, there is no Lorentz force, so more

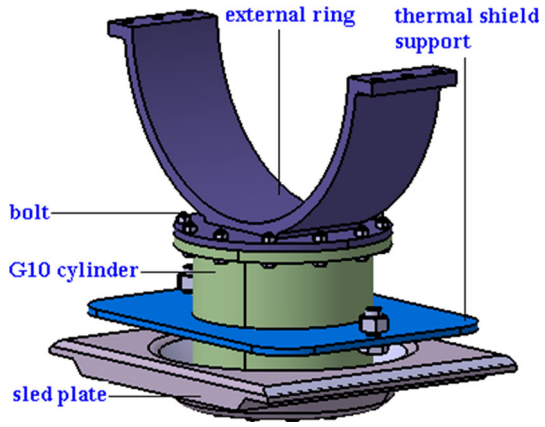

Fig. 8 3-D model of cold mass support on CFT

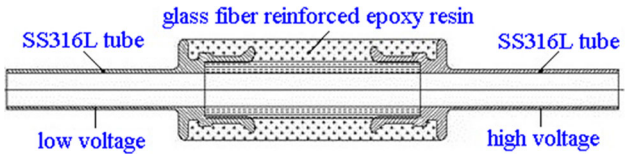

Fig. 9 Schematic diagram of axial insulator

attention should be paid on thermal design. As shown in Fig. 2, the thermal conductivity of G10 is much lower than SS, therefore, G10 is chosen to develop the cylinder, and SS is chosen to develop external ring, sled plate, bolts and nuts. The external ring, cylinder and sled plate are connected by bolts with nuts [7].

Considering the difference of coefficient of thermal expansion, the bolts with nuts used to connect external ring, cylinder and sled plate will loosen during cool down, so one bolt will be pretightened with two nuts and a spring gasket. In addition, to reduce thermal radiation through G10 cylinder, a multi-layer insulation system made of glass fiber and aluminium foil is horizontal set inside the G10 cylinder.

Insulator

Insulators play an important role in insulating the cryopipes [8–13], as shown in Fig. 1. Due to brittleness of ceramic insulator in cryogenic temperature, ceramic insulator for fusion device is gradually replaced with glass fiber reinforced epoxy resin composite insulator. On the structure, a composite insulator for STR-3 feeder consists of two SS316L tubes and glass fiber reinforced epoxy resin composite, as shown in Fig. 9.

According to working requirements, the leakage current of composite insulator for STR-3 feeder under 35 kV

Table 3 Element type

Items	Parameters
Cryopipe	Pipe16
Separator plate, terminal box	Shell181
Containment duct	Shell181
ICF support	MPC184
Sliding plate of the cold mass support	Solid185
Cylindrical of the cold mass support	Beam188
Contact between cryopipe and its support	Conta178
Contact between cold mass support and its rail	Conta173, targe170

voltage and 4.5 K temperature should be lower than 5 μA, in addition, the leakage rate under 4 MPa helium pressure should be lower than 1.0×10^{-9} Pa·m^3/s.

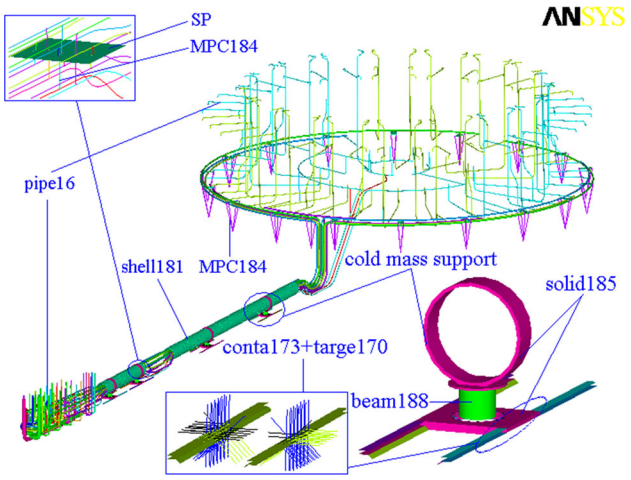

Fig. 10 The FE model of STR-3 feeder

Structural Design Criteria

Due to low out-gassing rate, low magnetic permeability and excellent cryogenic mechanical properties, SS304L, SS316L, copper, G10 and 3003 aluminium alloy are chosen as the main structural material to construct STR-3 feeder, the properties of SS304L/316L and copper are listed in Tables 1 and 2.

According to the structural design criteria from the ITER organization (IO) in Cadarache, southern France [14], the reliability and safety of STR-3 feeder under normal working condition will be evaluated based on the structural analysis. The allowable stress S_m is decided by

$$S_m = \frac{2}{3} S_y \tag{7}$$

where S_y is yield strength. The allowable stresses of SS304L and SS316L are listed in Table 1.

Additionally, if P_m is general membrane stress, P_b is primary bending stress, the relations should satisfy (8)–(9)

$$P_m \leq S_m. \tag{8}$$

$$P_m + P_b < 1.5 S_m. \tag{9}$$

Structural Analysis of Global Model

Global Finite Element Model, Loads and Boundary Conditions

To simulate the structural behavior under normal working condition, the static analysis is performed based on combination of computer aided design (CAD) [15] and finite element (FE) technology. The FE model is established according to the 3-D model. Firstly, the central lines of cryopipes, and the middle surfaces of separator plate (SP) and containment duct (CD) are extracted in CATIA V5, then, the global FE models are established by ANSYS Parametric Design Language (APDL) based on the extracted central lines and middle surfaces, moreover, the 3-D models of cold mass supports are imported from CATIA V5 to ANSYS, all the chosen elements to establish the FE models are listed in Table 3.

As shown in Fig. 10, the global FE model includes cryopipes, SP and CD with four cold mass supports, the insulators used to connect cryopipes are simplified. The structural analysis of TB will be performed after the global analysis. To simplify the FE model of ICF, 4 MPC184 elements are used to simulate one support for cryopipes fixed on coils cases. And MPC184 elements are also used to simulate the rigidity supports between the cryopipes and SPs too. The load cases of structural analysis of global model are as follows [16].

Case 1: Gravity

Case 2: Gravity + helium pressure + cool down + coils cases displacements

Due to vacuum inside cryostat of CFT, the cryostat suffers pressure difference and gravity. Considering there is no cryostat in the FE model, so the pressure difference in structural analysis of global model won't be taken into account. Conta178 and Conta173 elements are used to simulate sliding of cryopipes and cold mass supports during cool down and warm up. The defined coefficient of friction is 0.1. In the structural analysis, one global Cartesian coordinate and one global cylindrical coordinate are employed [17]. For the former one, the central line of CFT is placed on the Y axis, the Z axis points in the vertical direction upwards, and the X axis means to the side of the CFT. For the latter one, the Z axis is the same with the Cartesian one, the X axis means the radius, and the Y axis means tutorial angle.

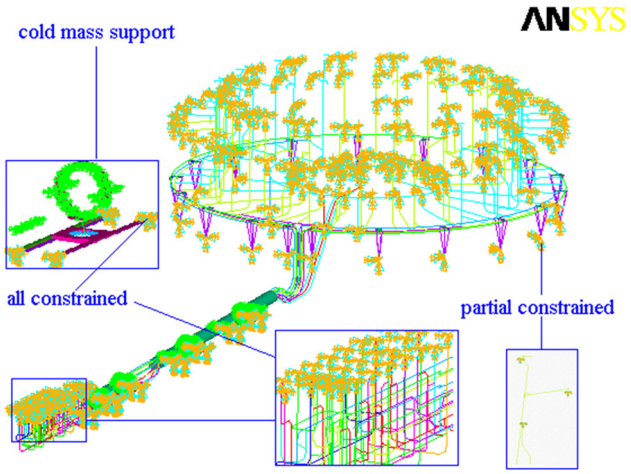

Fig. 11 Loads and boundary conditions

The applied radial, tangential and vertical displacements of ICF supports on TF coils cases are −25 mm, 11 mm and −7 mm respectively, and the displacements of end joints of cryopipes are obtained according to the displacements of corresponding magnets. In addition, the applied current temperature, reference temperature, internal pressure of cryopipes and acceleration of gravity are 4.5 K, 293 K, 6 bar and 9.8 m/s^2 respectively. After the fixed dovetails of cold mass supports and the ends of cryopipes on TB are constrained completely, the FE model of STR-3 feeder are as shown in Fig. 11.

Results

As shown in Fig. 12, it can be clearly seen that the displacements of ICF are higher, which mainly come from the cold-contraction and the external displacements loads of coils cases. Without considering the stress concentration of cold mass support, the peak stress intensity of cryopipes is 280 MPa, as shown in Fig. 13, which is lower than the allowable stress 287 MPa. For engineering consideration, the cryopipes should have enough mechanical strength in terms of safety margin, therefore, S bends or U bends on cryopipes are necessary.

From Fig. 14, it is found that the lowest reaction force of the end of cryopipes located at TB is 58.11 N, however, the maximum reaction force is 2.44 kN. To reduce the reaction force and protect STR-3 feeder system, it is necessary to use multi-bends on cryopipes near TB.

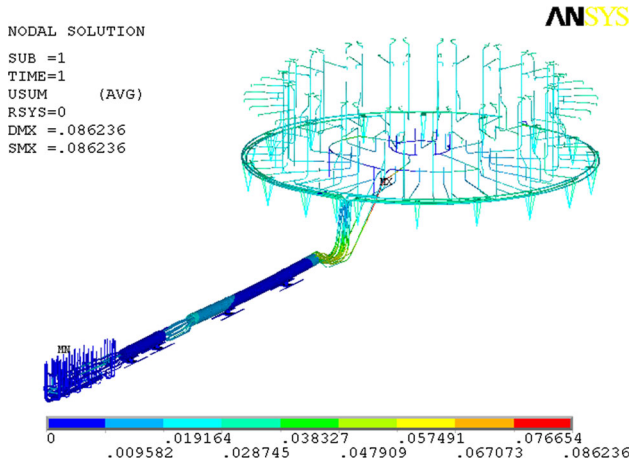

Fig. 12 Displacements (unit: meters)

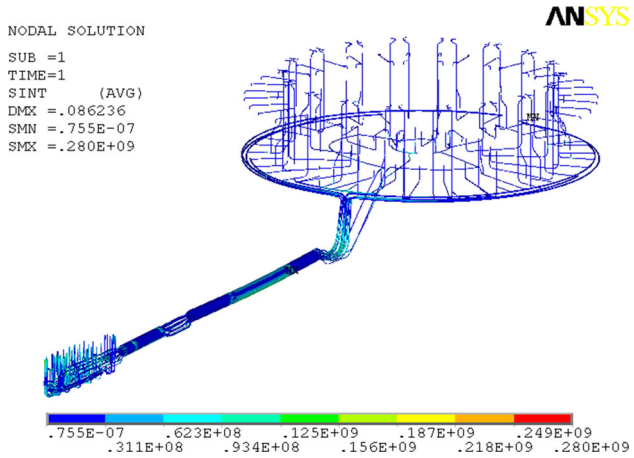

Fig. 13 Stress intensity of the cryopipes and CD (unit: pascals)

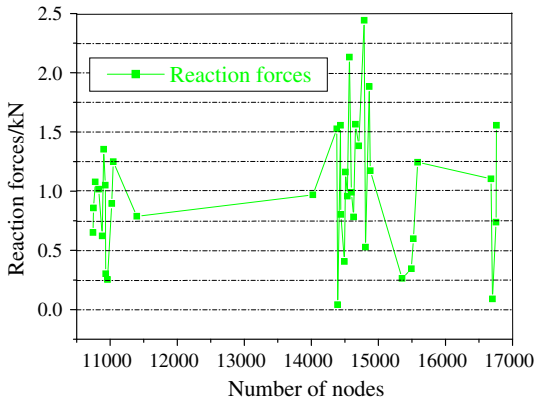

Fig. 14 Reaction forces of the valves ports

Structural Analysis of Terminal Box

As a key component, TB is used to hold the thermal shield, cryopipes and other cold mass. To reduce the heat leakage, vacuum environment inside TB is required. However, once the coolant is leaked into the vacuum space, TB will suffer overpressure and easy to be damaged. Therefore, it is necessary to perform the structural analysis of TB under over-pressure, which corresponds to 0.3 MPa inside TB and 0.1 MPa outside TB, so the pressure difference is

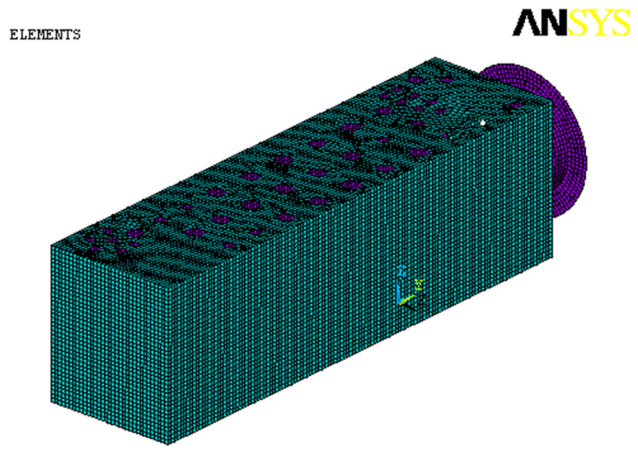

Fig. 15 Finite element model

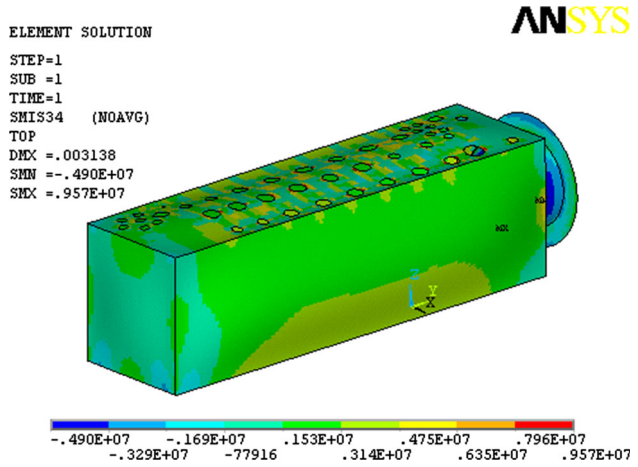

Fig. 16 Membrane stresses (unit: pascals)

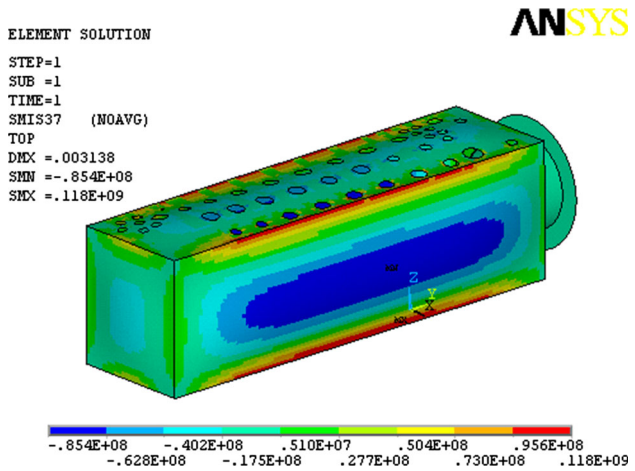

Fig. 17 Bending stresses (unit: pascals)

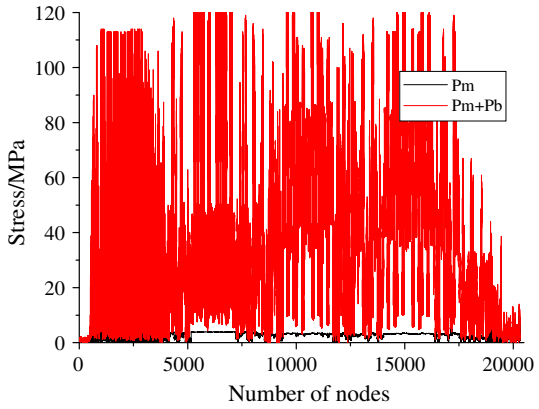

Fig. 18 Pm, Pm + Pb of terminal box

0.2 MPa. Figure 15 is the FE model of TB, the positions of 4 ground supports are fully constrained. When the wall thickness of TB is 40 mm, Figs. 16 and 17 are membrane stresses and bending stresses distribution respectively.

Obviously, the peak bending stress is much higher than peak membrane stress, the stresses concentration are at the right-angled corners. Undoubtedly, arc corner should be used to reduce stress concentration.

P_m, $P_m + P_b$ of TB is as shown in Fig. 18. For SS304L, the yield strength is 170 MPa at 293 K. According to formulas (7)–(9), S_m is 113 MPa, $P_m < S_m = 113$ MPa, $P_m + P_b < 1.5S_m = 170$ MPa, consequently, TB is safe under overpressure. To improve the safety margin, ribs can be welded on the surfaces of TB.

Buckling Analysis of Terminal Box

Buckling analysis is used to determine critical outer loads at which TB becomes unstable [18]. Therefore, a unit outer pressure is specified, the corresponding deformed shape of No. 1 mode is as shown in Fig. 19. Because the load factors represent the buckling loads, Fig. 19 indicates the critical loads are much higher than 0.1 MPa, which corresponds to the pressure difference under normal working condition. Buckling analysis indicates the stability of TB is enough.

Discussion

As one of the key system of ITER project, STR-3 feeder plays an important role in maintaining the safe and stable running of superconducting magnets. The combination of 3-D model and APDL is used to establish FE model of cryopipes, SP and CD, in addition, the superposition principle is used to create the globe FE model. Undoubtedly, this method can be used to perform other large scale analysis.

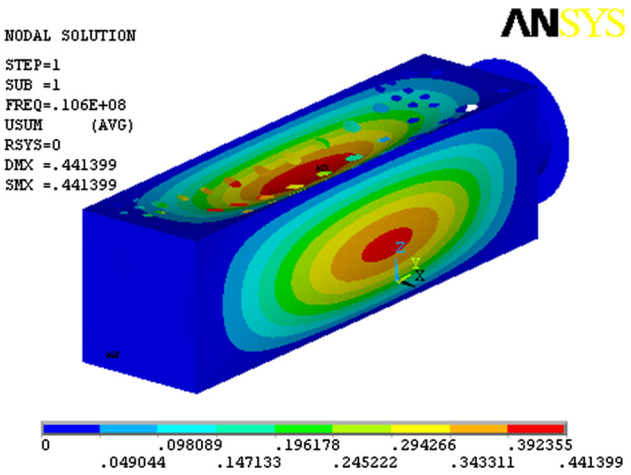

Fig. 19 Deformed shape of No. 1 mode (outer pressure)

According to the simulating results, when the stress concentration is considered, it is very necessary to enhance the flexibility of cryopipes. In particular, due to shearing force and other unfavorable loads, a number of insulators on ICF maybe suffer damage. Therefore, in the following engineering design, more attention should be paid on reducing the reaction force on the insulators.

Actually, the distance between thermal shield and TB is too small, so the length of the supports between them is small too, which leads to high heat leakage, in order to reduce the operating costs, more attention should be paid on the structural design of supports between thermal shield and TB.

Summary and Conclusion

1. The structural analysis indicate S bend or U bend near TB is necessary, which can reduce the reaction force of valve ports, so further structural optimization is needed from the engineering point of view.
2. Though the mechanical strength and stability of TB is enough, in order to improve the safety margin, arc corners and ribs are necessary.
3. Additional areas, including reducing the heat leakage to cryopipes, high voltage insulation, radiation of composite insulation materials, overpressure protection and seismic analysis [19–24], need to be investigated further.

Acknowledgments The authors would like to thank the related experts of the ITER organization (IO) supported by China, European Union, India, Japan, Korea, Russia, and the U.S., and the experts of Altair Engineering Inc and so on. The views and opinions expressed in this paper do not necessarily reflect those of IO. This work was supported by the National Basic Research Program of China (973 Program) (Grant No. 2008CB717900), the Special Fund of Talent Development of Anhui Province (Grant No. 2009Z056) and the Fund of Anhui Educational Committee (Grant Nos. KJ2013A072, KJ2011Z054).

References

1. M. Ferrari, P. Barabaschi, C.T.J. Jong, Y. Krivchenkov, R.K. Maix, N. Mitchell, Design optimisation of the ITER TF coil case and structures. Fusion Eng. Des. **75–79**, 207–208 (2005)
2. Y. Song, P. Bauer, Y. Bi, Y. Chen, Y. Cheng, A. Devred et al., Design of the ITER TF Magnet Feeder Systems. IEEE Trans. Appl. Supercond. **20**, 1710–1713 (2010)
3. B. Giesen, A. Panin, T. Boguszewski, S. Brons, A. Charl, G. Czymek et al., Structural evaluation of the busbar system of Wendelstein 7-X stellarator. Fusion Eng. Des. **82**, 1591–1598 (2007)
4. Y. Zhu, Y. Song, Y. Zhang, Z. Wang, Conceptual design and analysis of cold mass support of the CS3U feeder for the ITER. Plasma Sci. Technol. **15**, 599–604 (2013)
5. Y. Zhu, C. Liu, X. Liu, W. Wu, S. Wu, Design and analysis of the thermal shield of the prototype superconducting dipole magnet for GSI. IEEE Trans. Appl. Supercond. **23**, 4001108 (2013)
6. Y. Zhu, S. Wu, W. Wu, H. Xu, C. Liu, Design and heat load analysis of support structure of CR superconducting dipole superconducting magnet for FAIR. Nucl. Fusion Plasma Phys. **28**, 218–222 (2008). (In Chinese)
7. K. Lu, Y. Song, E. Niu, T. Zhou, Z. Wang, Y. Chen et al., Evolution of the design of cold mass support for the ITER magnet feeder system. Plasma Sci. Technol **15**, 196–200 (2013)
8. H. Liu, Q. Qu, Q. Pan, Y. Wu, C. Huang, L. Li et al., Testing of the ceramic insulation break for fusion device. IEEE Trans. Appl. Supercond. **24**, 7700204 (2014)
9. S. Fink, W.H. Fietz, G. Kraftb, H. Scheller, E. Urbach, V. Zwecker, Paschen testing of ITER prototype cryogenic axial breaks. Fusion Eng. Des. **88**, 1475–1477 (2013)
10. Klaus-Peter Weiss, Elisabeth Urbach, Günter Kraft, Holger Scheller, Cryogenic mechanical testing of ITER prototype axial breaks. Fusion Eng. Des. **88**, 1533–1536 (2013)
11. W.H. Fietz, S. Fink, G. Kraft, H. Scheller, E. Urbach, V. Zwecker, High Voltage Testing of ITER Prototype Axial Breaks. IEEE Trans. Appl. Supercond. **23**, 4200604 (2013)
12. D.P. Ivanov, B.N. Kolbasov, I.O. Anashkin, P.P. Khvostenko, W.J. Pan, S. Pradhan et al., Operational experience with forced cooled superconducting magnets. Fusion Eng. Des. **88**, 1569–1575 (2013)
13. D. Evans, Turn, layer and ground insulation for superconducting magnets. Phys. C, Supercond. **354**, 136–142 (2001)
14. C. Jong, N. Mitchell, A. Alekseev, *ITER magnet structural design criteria part I: main structural components and welds [R]* (ITER Org, Cadarache, 2008)
15. C. Liu, D. Yao, X. Fan, L. Li, Z. Wang, Z. Zhou et al., The design and analysis of the cooling system of NBI thermal shielding for EAST A# equatorial port. J. Fusion Energ. **33**, 382–385 (2014)
16. S.W. Zhang, Y.T. Song, Z.W. Wang, H. Jin, S.S. Du, X. Ji et al., Structural and fracture mechanics analysis for the bracket of iter upper elm coil. J. Fusion Energ. **33**, 304–308 (2014)
17. S.W. Zhang, Y.T. Song, Z.W. Wang, X. Ji, S.S. Du, Struc tural design study for ITER upper ELM coils. J. Fusion Energ. **33**, 184–188 (2014)
18. V. Bykov, F. Schauer, K. Egorov, A. Tereshchenko, P. van Eeten, A. Dübner et al., Structural analysis of W7-X: Overview. Fusion Eng. Des. **84**, 215–219 (2009)
19. P.P. Granieri, M. Breschi, M. Casali, L. Bottura, A. Siemko, Thermo-electric analysis of the interconnection of the LHC main superconducting bus bars. Cryogenics **53**, 107–118 (2013)

20. Kerstin Rummel, Andre John, Insulation of the coil and bus bar ends during assembly of W7-X. IEEE Trans. Appl. Supercond. **16**, 751–754 (2006)
21. Holger Scheller, Hans-Peter Langenberg, Michael Kühnberg, Jürgen Baldzuhn, Boy Petersen-Zarling, Dirk Gustke et al., Paschen testing on W7-X coils and components in the BNN test facility. IEEE Trans. Appl. Supercond. **16**, 759–762 (2006)
22. C.S. Wei, W.J. Pan, S.H. Sun, H.W. Liu, Irradiation effects on a glycidylamine epoxy resin system for insulation in fusion reactor. J. Nucl. Mater. **429**, 113–117 (2012)
23. Z. Wu, J. Li, C. Huang, R. Huang, L. Li, Processing characteristic and radiation resistance of various epoxy insulation materials for superconducting magnets. Fusion Eng. Des. **88**, 3078–3083 (2013)
24. Jean-Philippe Girard, Gottfried Grünthal, Marc Nicolas et al., Design earthquakes for ITER in Europe at Cadarache. Fusion Eng. Des. **75–79**, 1109–1113 (2005)